

Neutron star mass limit at $2M_{\odot}$ supports the existence of a CEP

D. Alvarez-Castillo^{1,a}, S. Benic^{2,b}, D. Blaschke^{1,3,4}, Sophia Han^{5,6}, and S. Typel⁷

¹ Bogoliubov Laboratory of Theoretical Physics, JINR Dubna, Dubna, Russia

² Department of Physics, University of Zagreb, Zagreb, Croatia

³ National Research Nuclear University (MEPhI), Moscow, Russia

⁴ Institute of Theoretical Physics, University of Wrocław, Wrocław, Poland

⁵ Department of Physics and Astronomy, University of Tennessee, Knoxville, TN 37996, USA

⁶ Physics Division, Oak Ridge National Laboratory, Oak Ridge, TN 37831, USA

⁷ GSI Helmholtzzentrum für Schwerionenforschung GmbH, Darmstadt, Germany

Received: date / Revised version: date

Abstract. We point out that the very existence of a "horizontal branch" in the mass-radius characteristics for neutron stars indicates a strong first-order phase transition and thus supports the existence of a critical endpoint (CEP) of first order phase transitions in the QCD phase diagram. This branch would sample a sequence of hybrid stars with quark matter core, leading to the endpoint of stable compact star configurations with the highest possible baryon densities. Since we know of the existence of compact stars with $2M_{\odot}$, this hypothetical branch has to lie in the vicinity of this mass value, if it exists. We report here a correlation between the maximal radius of the horizontal branch and the pressure at the onset of hadron-to-quark matter phase transition which is likely to be a universal quantity of utmost relevance to the upcoming experiments with heavy-ion collisions at NICA and FAIR.

PACS. 97.60.Jd Neutron stars – 26.60.Kp Equations of state for neutron star matter – 12.39.Ki Relativistic quark model

1 Introduction

The study of the internal composition of neutron stars (NS) is an active field of research which relies on astrophysical observations that allow to refine theoretical models. Matter inside neutron star interiors is so dense that nuclear interactions must be taken into account. Fundamental properties like the maximum neutron star mass and radius are determined by their internal composition, namely the equation of state (EoS). Recent observations of massive NS [1, 2, 3] resulted not only in constraints on the stiffness of the EoS, but also in a reduction of the densities reached in the center of a massive NS. The stiffer the high-density EoS, the higher the maximum mass supported by it and the flatter the density profile of the compact star interior. Furthermore, the possibility of deconfined quark matter content inside NS can be an indication for a critical endpoint (CEP) in the QCD phase diagram if the deconfinement process occurs via a strong first phase transition. In the other hand, in order to prove the existence of a CEP in the QCD phase diagram, it is sufficient to demonstrate that at zero temperature $T = 0$ a first order phase

transition exists as a function of the baryochemical potential μ , since it is established knowledge from ab-initio lattice QCD simulations that at $\mu = 0$ the transition on the temperature axis is a crossover. Moreover, the appearance of a gap in the mass-radius relationship for compact stars leads to the phenomenon known as third family (aka "mass twins") which will imply that the $T = 0$ equation of state of compact star matter exhibits a strong first order transition with a latent heat, that for the EoS scheme presented in [26] satisfies $\Delta\varepsilon/\varepsilon_{\text{trans}} > 0.6$, where $\varepsilon_{\text{trans}}$ is the critical energy density and $\Delta\varepsilon$ the latent heat of the transition. Since such a strong first order transition under compact star conditions will remain first order when going to symmetric matter, the observation of a disconnected branch (also known as third family) of compact stars in the mass-radius ($M - R$) diagram proves the existence of a CEP in QCD.

A very important ingredient in the microscopic description of hadronic matter is the interactions between the quarks confined inside baryons as densities increase towards the phase transition. These effects are described by an effective excluded volume of baryons that go beyond the simple point-like description and the result is a stiffening of the hadronic EoS. Once deconfinement has set in, these quark interactions shall start to increase therefore leading to multiquark interactions that will eventually

Send offprint requests to:

^a On leave from: Instituto de Física, Universidad Autónoma de San Luis Potosí, México

^b Present address: University of Tokyo, Tokyo, Japan

stiffen the quark EoS and will stabilize the third branch in the $M - R$ relation right after the gap that separates the second branch. As we will see in the next sections, the high mass twins require an EoS that is stiff both in the hadronic phase, as well as in the quark phase in order to stabilize the hybrid star solutions, located in the third branch in the $M - R$ diagram. This result is on contrast to other approaches to quark matter, like CFL solutions in the NJL model [5, 4], or holographic descriptions [6], where the hadron-quark matter transition leads to an instability against radial oscillations, collapsing the compact star.

A different approach leading to a crossover for hadronic and quark matter is the so called *three window approach* [7]. It is characterized by the use of percolated quark matter equations of state at high density where as in the intermediate domain matter is described by an interpolation between the low density hadronic matter and the high density quark matter. The percolation mechanism is the result of the three window domain of quark matter interactions: a) few quark exchange at densities below $2n_0$, b) many-quark exchange resulting in a structural change of hadrons at about $2n_0 < n < 5n_0$ and c) baryon overlap namely baryon percolation and Fermi sea development for $n > 5n_0$. The resulting neutron stars can be as stiff as the observed $2 M_\odot$, however under this scheme the third branch and the high mass twins will not appear.

It is important to mention that in [8] based on the symmetries of the QCD Lagrangian, it has been suggested that cold dense baryonic matter would undergo a continuous transition to quark matter and thus a first order phase transition should not be expected for $T=0$ matter. These considerations got supported by [9], where it had been found that the Kobayashi-Maskawa-'t Hooft determinant interaction describing the axial anomaly of QCD would correspond by Fierz transformation to an effective repulsive interaction induced by a six-quark vertex coupling to diquark condensates which in effective quark matter models of the NJL type leads to a second critical endpoint at low temperatures, below which the hadron-to-quark matter transition would become a crossover, see also [10]. If, however, the horizontal branch of the neutron star $M - R$ diagram would be observed in nature, these ideas of a quark-hadron continuity must be revised!

We have already underlined the importance of the high-mass twin stars phenomenon in the framework of the nature of the QCD phase diagram. However, there are other aspects that are also covered, namely solutions to the hyperon puzzle [11], the masquerade problem [12] and the reconfinement case [13, 14].

As for the Astronomy front, upcoming observations from NICER [15] and SKA [16] it shall be possible to detect high mass NS twins. Bayesian Analysis (BA) studies are useful to assess the possibility of their identification. Several results can be found in [17, 18, 19, 20, 21, 22], where disjunct $M-R$ constraints have been used for extracting probability measures for hybrid NS EoS. In the most recent paper [17], consideration a fictitious radius measurement of both the pure hadronic NS and the corresponding hybrid twin has brought interesting results. By means of

BA, the authors performed model discrimination and obtained the most reliable parameters related to the highest probabilities. These results are of great importance to the observers since they provide a guidance for astronomical data filtering.

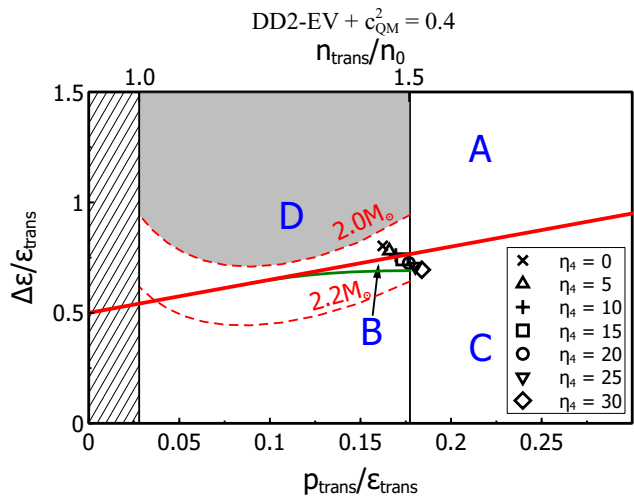


Fig. 1. Properties of the hybrid NS EoS. The EoS in the figure corresponds here is composed of the hadronic DD2 that includes excluded volume corrections together with the NJL model with multiquark interactions, see section 2.2.2. The regions are classified according to [26], where the $M - R$ configurations have a stable hybrid star branch that can be: (D)isconnected from the hadronic branch, (C)onnected with it, (B)oth or (A)bsent.

This work is organized as follows: In section 2 we review different approaches to the high mass twin EoS, exposing the main features of each model. In section 3 we make the connection with Astrophysics by summarizing the most relevant astrophysical cases and observables related to the high mass twins. In section 4 we discuss the overall picture and finally we present our results and enumerate the physical inputs for the NICA experiment resulting from the twins phenomenon just before the final conclusions section.

2 Hybrid compact star EoS models with strong first order phase transition.

In this section we review several approaches to the dense matter EoS that undergo a strong first-order transition between the hadron and quark regions, describing the high mass twin phenomenon. The resulting massive hybrid neutron stars are composed of a hadronic mantle with quark matter cores and are located in the third branch of the $M - R$ diagram, where each curve represents sequences of static, non-rotating, compact stars for a given EoS after solution of the TOV equations [23, 24].

The hadronic NS EoS description includes excluded volume corrections that are applied at densities higher than saturation in order to respect the empirical values obtained from diverse laboratory measurements.

The excluded volume correction is applied at suprasaturation densities and has the effect of stiffening the EoS without modifying any of the experimentally well constrained properties below and around saturation $n_{\text{sat}} = 0.16 \text{ fm}^{-3}$, the density in the interior of atomic nuclei.

In [17] the DD2 and DD2F EoS features this correction by considering the available volume fraction Φ_N for the motion of nucleons as density dependent n as introduced in [25]

$$\Phi_N = \begin{cases} 1, & \text{if } n \leq n_{\text{sat}} \\ \exp[-v|v|(n - n_{\text{sat}})^2/2], & \text{if } n > n_{\text{sat}} \end{cases}, \quad (1)$$

where $v = 16\pi r_N^3/3$ is the van-der-Waals excluded volume for a nucleon with a hard-core radius r_N . To complete the hybrid NS EoS, a quark matter (QM) EoS is to be included through a phase transition, therefore in the following subsections a brief description of the different approaches to the QM EoS is presented.

2.1 ZHAHP scheme

This approach [14, 26] is based on an EoS ansatz for the description of quark matter, characterized by a constant speed of sound c_{QM} . While keeping the hadronic equation of state fixed, the strength of the first order phase transition $\Delta\varepsilon$ is varied and the resulting $M - R$ curves are studied. The EoS takes the following form:

$$\varepsilon(p) = \begin{cases} \varepsilon_H(p), & p < p_{\text{trans}} \\ \varepsilon_{\text{trans}} + \Delta\varepsilon + c_{QM}^{-2}(p - p_{\text{trans}}), & p > p_{\text{trans}} \end{cases} \quad (2)$$

where $\varepsilon_H(p)$ is the hadronic EoS, p_{trans} is the pressure at the phase transition and $\varepsilon_{\text{trans}} = \varepsilon_H(p_{\text{trans}})$ is the energy density at the onset of the phase transition. Variations of the three parameters p_{trans} , $\Delta\varepsilon$ and c_{QM} lead to different sequences of compact star configurations in the $M - R$ diagram. According to [26] the $M - R$ configurations have a stable hybrid star branch that can be: (D)isconnected from the hadronic branch, (C)onnected with it, or (B)oth, see Fig. 1. The line

$$\frac{\Delta\varepsilon}{\varepsilon_{\text{trans}}} = \frac{1}{2} + \frac{3 p_{\text{trans}}}{2 \varepsilon_{\text{trans}}} \quad (3)$$

is shown in that figure and divides the cases (D) and (C). Sequences on that line exhibit an endpoint of hadronic configurations from which a "horizontal branch" of almost unstable hybrid stars begins. Such a horizontal branch would be a clearly detectable observational indication for a strong first order phase transition (since $\Delta\varepsilon > \varepsilon_{\text{trans}}$) which provides evidence for the existence of a CEP in the QCD phase diagram [27, 28].

2.2 Microscopic models of quark matter

In this section we provide a few examples of microscopic approaches to the quark matter EoS for which high-mass twin star solutions have been reported. They all belong to the meanfield level of description for which the grand canonical potential takes the generic form

$$\Omega = U + \Omega^{FG} - \Omega_0, \quad (4)$$

where U is a meanfield contribution and Ω_0 specifies the normalization of the thermodynamical potential of the vacuum. $\Omega^{FG} = \sum_{f=u,d,s} \Omega_f^{FG}(T, \tilde{\mu}_f; X)$ is the Fermi gas expression which can still depend on order parameters X to be determined in thermodynamic equilibrium from the solutions of the corresponding gap equations $\partial\Omega/\partial X = 0$. These fix, e.g., the masses and pairing gaps for quarks in dense matter. The EoS are then obtained the standard way

$$p = -\Omega, \quad -\frac{\partial\Omega}{\partial\mu_f} = n_f, \quad \varepsilon = -p + \sum_{f=u,d,s} \mu_f n_f. \quad (5)$$

After implementing the constraints of β -equilibrium and charge neutrality the EoS will depend only on one chemical potential which can be chosen as that corresponding to the baryon number.

2.2.1 Bag model with color superconductivity

An interesting hybrid NS EoS that includes color superconducting quark matter in the color flavor locked (CFL) phase has been given in [12] and was reported to possess high-mass twin star solutions in [29, 30].

At high densities, the CFL quark matter phase expected to be found in the core of hybrid stars. It is described within the Nambu-Jona-Lasinio (NJL) model augmented with perturbative QCD corrections and augmented with a background pressure. The grand canonical thermodynamic potential that takes the generic form of (4) is composed of the following expressions:

$$\Omega^{FG} = \sum_{f=u,d,s} \frac{3}{\pi^2} \int_0^{\sqrt{\mu_i^2 - m_i^2}} dp p^2 \left(\sqrt{p^2 + m_i^2} - \mu_i \right) \quad (6)$$

where the mass of the light quarks (u and d) is neglected and $m_s = 150 \text{ MeV}$. There is also a bag constant for the background field

$$\Omega_0 = -B, \quad (7)$$

and the mean field is given by

$$U = \frac{3}{4\pi^2} c \mu^4 - \frac{3\Delta^2 \mu^2}{\pi^2}, \quad (8)$$

where the term proportional to μ^4 corresponds to QCD inspired corrections with $c = 0.3$. The second term involving the CFL gap parameter Δ is the lowest order contribution from the CFL condensate formation. In this

approach, Δ is introduced by hand instead of being computed from the gap equations, in contrast with the other models, see for instance, [31]. This EoS is complemented with a Goldstone boson condensate that contributes to the total baryonic pressure. Moreover, the quark-hadron phase transition features a mixed phase where charge neutrality is enforced globally as well as the Gibbs conditions. The resulting neutron star configurations feature a third branch in the $M - R$ diagram as well as unstable quark configurations that bifurcate from the hadronic sequence. Hybrid stars have masses in the range $1.0 - 2.1 M_\odot$. Under this scheme, the $2M_\odot$ NS is realized with the following choice of parameter values

$$\Delta = 50 \text{ MeV}, \quad B^{1/4} = 218 \text{ MeV}.$$

The hadronic phase EoS implemented in this model is based on the extended FTRMF model [32] that includes contribution from self-interactions and mixed terms for mesons up to fourth order, but *it does not* include excluded volume corrections.

2.2.2 NJL model with multi-quark interactions

Within this approach, the EoS in the high density phase is computed by means of a NJL model with multi-quark interactions [33,34]. The thermodynamic potential functions are

$$U = 2 \frac{g_{20}^2}{\Lambda^2} (\phi_u^2 + \phi_d^2) + 12 \frac{g_{40}^2}{\Lambda^8} (\phi_u^2 + \phi_d^2)^2 - 2 \frac{\eta_2 g_{20}}{\Lambda^2} (\omega_u^2 + \omega_d^2) - 12 \frac{\eta_4 g_{40}}{\Lambda^8} (\omega_u^2 + \omega_d^2)^2, \quad (9)$$

where the following shifts apply

$$M_u = m + 4 \frac{g_{20}}{\Lambda^2} \phi_u + 16 \frac{g_{40}}{\Lambda^8} \phi_u^3 + 16 \frac{g_{40}}{\Lambda^8} \phi_u \phi_d^2, \quad (10)$$

$$\tilde{\mu}_u = \mu_u - 4 \frac{g_{02}}{\Lambda^2} \omega_u - 16 \frac{g_{04}}{\Lambda^8} \omega_u^3 - 16 \frac{g_{04}}{\Lambda^8} \omega_u \omega_d^2, \quad (11)$$

where the same relations hold for the down quark quantities by interchanging the indices d and u . The parameters of the model are computed by means of finding the extremum value of the thermodynamic potential (4) with respect to the mean-fields ($X = \phi_u, \phi_d, \omega_u, \omega_d$), i. e. The intensity of the vector channels is quantified by the ratios

$$\eta_2 = \frac{g_{02}}{g_{20}}, \quad \eta_4 = \frac{g_{04}}{g_{40}}. \quad (12)$$

The parameter η_4 determines the stiffness of the quark matter EoS at high densities, a very important behavior for the stability of the third branch in the $M - R$ diagram.

$$\frac{\partial \Omega}{\partial X} = 0, \quad (13)$$

and as usual, the pressure is obtained from the relation $p = -\Omega$ with charge neutrality and β -equilibrium enforced in the standard way. For more details, see [33]. The hadronic part of the EoS is taken to be the DD2

model with excluded volume correction [33] and a Maxwell construction for the hadron-quark phase transition is implemented. High mass twins are found for $\eta_2 = 0.08$, $\eta_4 = 5, 6, 7, 8, 9$ and $v = 6 - 8 \text{ fm}^3$ (p60 - p80). The lower row of figure 2 shows high mass NS twins together with the corresponding parameter set.

2.2.3 Non-local quark matter model

The nonlocal PNJL model [35,36] describing the quark phase features a 4-momentum dependent form factor that is adjusted to describe the dynamical mass function as well as the wave function renormalization of the zero temperature propagator based on lattice QCD simulations [37, 38]. Moreover, the vector meson coupling η_v is set to reproduce the slope of the chemical potential dependence of the pseudocritical temperature $T_c(\mu)$ as obtained by lattice QCD calculations [39]. Unlike the other approaches, for the non-local model the Fermi-Matsubars sums cannot be computed analytically, therefore the mean fermion contribution reads

$$\Omega^{\text{FG}} = -4T \sum_{n,c} \int \frac{d^3 \mathbf{p}}{(2\pi)^3} \ln \left[\frac{(\tilde{\rho}_{n,\mathbf{p}}^c)^2 + M^2(\tilde{\rho}_{n,\mathbf{p}}^c)}{Z^2(\tilde{\rho}_{n,\mathbf{p}}^c)} \right], \quad (14)$$

with

$$M(p) = Z(p) [m + \sigma_1 g(p)], \quad Z(p) = [1 - \sigma_2 f(p)]^{-1}.$$

Here, instead of a four momentum variable the quantity

$$(\tilde{\rho}_{n,\mathbf{p}}^c)^2 = [\omega_n - i\tilde{\mu} + \phi_c]^2 + \mathbf{p}^2, \quad (15)$$

occurs which contains the Fermi-Matsubara frequencies $\omega_n = (2n+1)\pi T$, the chemical potential μ and the Polyakov loop variable Φ_c , where

$$\tilde{\mu} = \mu - \omega g(p) Z(p). \quad (16)$$

For details, see [40]. The mean field potential contains scalars (σ_1, σ_2) and vector (ω) gaps as well as a coupling to the traced Polyakov loop Φ_c which represents the homogeneous gluon background field ϕ_3 .

$$U = \frac{\sigma_1^2 + \kappa_p^2 \sigma_2^2}{2 G_S} - \frac{\omega^2}{2 G_V} + \mathcal{U}(\Phi, T, \mu), \quad (17)$$

with a μ -dependent logarithmic effective potential included:

$$\mathcal{U}(\Phi, T, \mu) = (a_0 T^4 + a_1 \mu^4 + a_2 T^2 \mu^2) \Phi^2 + a_3 T_0^4 \ln(1 - 6\Phi^2 + 8\Phi^3 - 3\Phi^4), \quad (18)$$

for the parameter values $a_0 = -1.85$, $a_1 = -1.44 \times 10^{-3}$, $a_2 = -0.08$, $a_3 = -0.40$. Polyakov loop potential \mathcal{U} contains an explicit dependence on the chemical potential μ so that an effect like the renormalization of the kinetic pressure term by perturbative QCD effects (proportional to the constant c in section 2.2.1 is effectively accounted for.

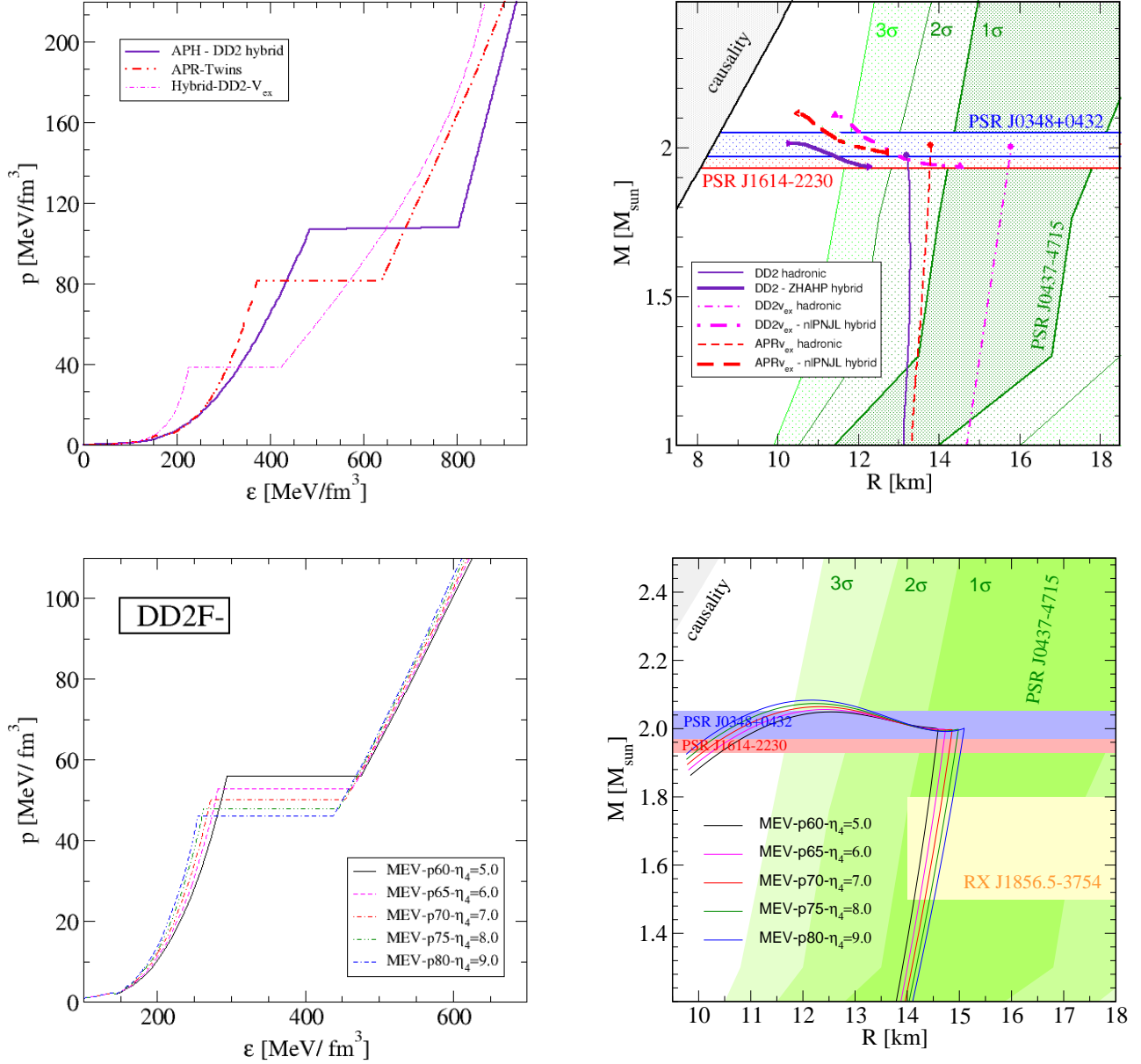


Fig. 2. Left column: High mass NS twins EoS. Right column: Corresponding mass-radius diagram for the high mass NS twins EoS. The almost vertical branch of purely hadronic stars is separated from the upper horizontal hybrid star branch by an unstable branch. Different branches to the high mass twins are presented in the upper figures, whereas the lower ones display a variation of parameters for the DD2-MEV with hNJL [33]. The recently measured masses for two $2 M_\odot$ pulsars are shown by red and blue hatched regions. Furthermore, the pressure at the phase transition p_{trans} on the EoS diagram is proportional to the NS radius in the MR plots, as can be read out from the figures.

In addition, the μ dependence of η_v is introduced by interpolating between zero temperature quark matter pressures $P_< = P_Q(\mu; \eta_<)$ and $P_> = P_Q(\mu; \eta_>)$ (under β -equilibrium conditions) which are calculated at different, but fixed values $\eta_< = \eta_v(\mu \leq \mu_c)$ and $\eta_> = \eta_v(\mu > \mu_c)$ [41]. From the Gibbs conditions, $P_H(\mu_c) = P_<(\mu_c)$, the critical chemical potential μ_c can be determined. The interpolation for hybrid NS matter is introduced in a Gaus-

sian form

$$P(\mu) = P_H(\mu)\Theta(\mu_c - \mu) + \frac{[(P_< - P_>) \exp[-(\mu - \mu_c)^2/\Gamma^2] + P_>] \Theta(\mu - \mu_c)}{(19)}$$

where $P_H(\mu)$ stands for the pressure of the hadronic phase in β -equilibrium. As with the other model approaches, the density jump at the first order phase transition is given by $\Delta n = \partial P_</\partial \mu|_{\mu=\mu_c} - \partial P_H/\partial \mu|_{\mu=\mu_c}$. Note that with the choice $\eta_< < \eta_>$ it is possible to achieve a strong first

order phase transition characterized by a large Δn allowing for stable hybrid star configurations at high central energy NS densities. High mass NS twins examples within this approach are shown in Fig. 2 (upper row) together with the ZHAHP scheme parametrization of Ref. [27]. Thus, the observation of the massive twins phenomenon would provide evidence for a strong first order phase transition in compact star matter.

2.2.4 Density functional approach (string-flip model)

Hybrid compact stars can be described by a excluded volume dependent EoS both in the hadronic and quark matter range. The string-flip model firstly introduced in [42, 43] allows for a description of quark-nuclear matter based on the confinement potential for the interactions between nearest neighbor quarks. In this section we present the approach developed in [44] which follows its relativistic form as introduced in [45] whose main ingredient is the reduction and vanishing of the effective string tension in dense matter, based on the multiquark interactions prescription. A two-flavor model is introduced with density dependence of the quark masses $m_I = \Sigma_s$, generated by the scalar quark selfenergy Σ_s (divergent as $n \rightarrow 0$) in order to produce deconfinement. Within the density functional approach (string-flip model), the zero temperature functional for the effective mass takes the form

$$M_f = M_{f_0} + D(n_s)n_s^{-\frac{1}{3}}, \quad (20)$$

where the last term is the confinement contribution. The function $D(n_s)$ is the effective in-medium string tension resulting from the product of the vacuum string tension, D_0 between quarks with an available volume fraction, $\Phi(n_s)$:

$$D(n_s) = D_0\Phi(n_s), \quad \Phi(n_s) = e^{-v^2 n_s^2}, \quad (21)$$

where v is the excluded volume parameter. The chemical potential is shifted as follows:

$$\tilde{\mu}_f = \mu_f - an_v - bn_v^3, \quad (22)$$

where n_v is the vector density. The mean field potential in this approach is given by

$$U = \frac{1}{3}D(n_s)n_s^{\frac{2}{3}} - 2v^2D(n_s)n_s^{\frac{8}{3}} + an_v^2 + 3n_v^4. \quad (23)$$

The first two terms arise from the string-flip model that includes available volume corrections while the two last ones represent repulsive multiquark interactions.

At lower densities the confinement interaction is expected to dominate, while the perturbative one gluon exchange interaction turns out to be more important at higher densities. A very important ingredient of this string-flip model is the effective in-medium string tension $D(n_B)$, which is the result of the product of the vacuum string tension $\sigma \sim D_0$ between quarks with the available volume fraction $\Phi(n_B)$. In this way, the excluded volume mechanism is active in both hadron and quark dense matter

phases. For the hadronic phase the DD2 model with excluded volume corrections is taken and the Maxwell construction is applied. High mass twin stars sequences are obtained in [44] for the parameters given there.

3 Mass-radius relations for high mass twins

$M - R$ measurements are important not only because it can be used as an indicator of hybrid compact stars, but of the existence of a CEP in the QCD diagram. In particular, the confirmation of a third branch disconnected from the hadronic neutron star branch suggested by several high mass twin models would support the existence of a first order phase transition, expected to be deconfinement. Due to limited accuracy of mass and radius measurements, such a third branch would reveal itself as a quasi horizontal part of the M-R relation at high mass. There exists also the possibility of the appearance of pasta phases at the interface between hadronic and quark matter in NS star interiors. A clear example is found in [46], where the authors consider different structural shapes at the boundary. Therefore, in [47] a study has been carried out with the purpose of testing the robustness of the high mass twins against pasta content by using an interpolation whose main parameter characterizes the pasta strength and it was found that for moderate values the twin phenomena remains. Thus, this study provides support for the robust existence of the high mass NS twins.

From the phenomenology of the massive hybrid stars and the third branch we can point out the following:

- (1) The hadronic phase should be stiff enough to reach the $2M_\odot$ measured NS. Excluded volume corrections can effectively account for it by stiffening the EoS.
- (2) The quark matter EoS can be soft around the quark-hadron phase interface region, especially when resulting in a strong first order phase transition, but should be stiffen up as density increases in order to maintain the stability of the third branch and result in the case D of figure 1.

4 Interplay between neutron star physics and heavy ion collisions

High mass NS twins scenario has been successfully described by different microscopic approaches to the EoS. We look into common features in this section. The EoS is characterized by a strong first order phase transition accompanied by a latent heat. The hadronic EoS is generally stiff while the quark matter description usually softens right after the transition and stiffens up at higher densities, providing the necessary stability for the compact stars that populate the third branch in the MR diagram.

From statistical models of particle production in heavy ion collisions, a universal transition pressure $p_{\text{trans}} = 82 \pm 8$ MeV/fm³ for the quark-gluon plasma (QGP) breakup and chemical freezeout is given in [48, 49]. This study covers the entire range of today's accessible reaction energies,

with $\sqrt{s_{NN}}$ ranging from 62.4 GeV to 2760 GeV. By looking at Fig. 3 we can associate a NS radius of 13.8 km for a high mass twin model with $p_{\text{trans}} = 80 \text{ MeV/fm}^3$. Fig. 3 shows a reciprocal relation between the NS radius and the pressure p_{trans} at the onset of quark matter in NS cores using the data from Fig. 2.

The fit formula for the relation between radius at $2M_\odot$ and transition pressure p_{trans} is

$$\frac{R}{10 \text{ km}} = 1.495 - 0.0021 \left(\frac{p_{\text{trans}}}{\text{MeV/fm}^3} - 22 \right) + \left(\frac{p_{\text{trans}}}{\text{MeV/fm}^3} - 31 \right)^{-1}. \quad (24)$$

An important quantity that related the EoS of symmetric matter with the NS EoS is the symmetry energy E_s , best determined by laboratory experiments around saturation density values than at high densities regions where at the present remains quite uncertain. The relevance of E_s for dense matter relies on the fact that it has a huge impact on the NS radius [51], allowing for a link between astrophysical observations and laboratory experiments. It has been recently conjectured in [53], that a *universal symmetry energy contribution to the NS EoS* exists, leading to the possibility of directly extracting the symmetric matter EoS from NS observations and vice versa.

5 Conclusions

From the investigation of the interrelations between the phenomenology of mass-radius relations for compact stars and the underlying equation of state for cold dense matter reviewed in this contribution, we can draw a few conclusions applying for the future HIC programmes at NICA, FAIR, low-energy RHIC and the possible heavy-ion collision program at J-PARC:

- (1) If the existence of a disconnected "third family" branch of compact stars in the M-R diagram (due to finite errors in the radius and mass measurements hardly distinguishable from a "horizontal branch") would be confirmed by observation, this would allow the conclusion that there must be a strong first order phase transition in the neutron star interior, most likely due to deconfinement.
- (2) A first order phase transition at $T=0$ in the QCD phase diagram would imply the existence of at least one critical endpoint: worth finding it in HIC experiments! If even in beta-equilibrium there is a first-order transition, it shall be there also in symmetric matter where there is less stress.
- (3) If a maximal radius of high-mass pulsars could be established this would provide a lower limit for the pressure at the onset of the phase transition in neutron star matter. This would provide an important constraint for the EoS models used in simulating and interpreting the heavy-ion collisions.

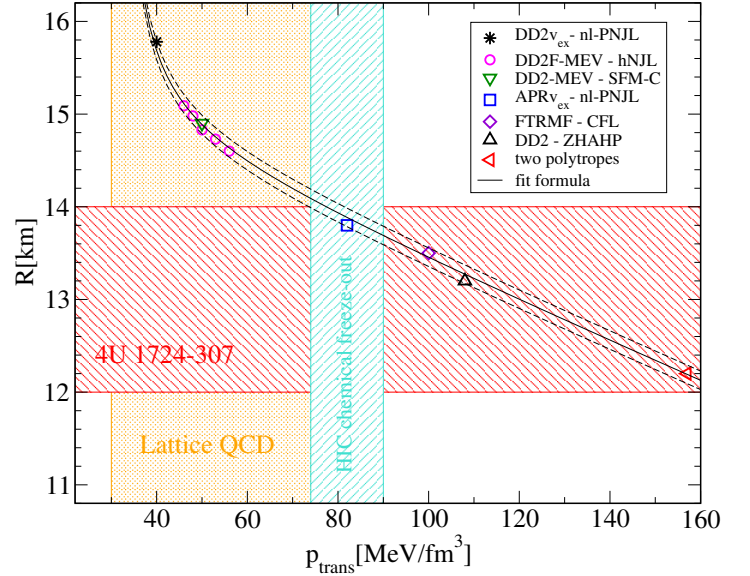


Fig. 3. NS Radius dependence on the p_{trans} for the models presented in figure 2. The square, the star and triangle-up symbols correspond to the models presented in [41], whereas the circles represent parameter values of the mass twin configurations in the framework of [33] extracted from Ref. [17]. Additionally, the diamond symbol is the result from the superconducting quark matter model [29], the triangle-down symbol stands for the string-flip model approach [44] and the triangle-left corresponds to the two polytropes EoS [54]. The shaded region represents results from Lattice QCD calculations for the crossover transition region [52], from a statistical model analysis of chemical freeze-out in heavy ion collisions that indicate a universal transition pressure [48, 49] and from a radius analysis for the X-ray burst spectra for the low-mass X-ray binary 4U 1724-307 [50]. Remarkably, the model with a radius $R_{\text{trans}} = 13.8 \text{ km}$ at onset of deconfinement is consistent with the universal transition pressure conjecture as well as with the recent radius measurement for the LMXB 4U 1724-307.

Already at present, without having observed yet the disconnected branch of high-mass twins in the M-R diagram, we may formulate an interesting conjecture, on the basis of our Fig. 3. Suppose the maximum radius ($\sim 14 \text{ km}$) of the range recently extracted from X-ray bursts of the compact star 4U 1724-307 by Suleimanov et al. [50] is such a maximum radius of hadronic compact stars, then the lower limit for the transition pressure would be at $\sim 80 \text{ MeV/fm}^3$. This is in striking agreement with the recently reported "universal" hadronization pressure from analyses of chemical freeze-out in HIC by Rafelski and Petran [48]. So we might conjecture that there is a universal limiting pressure of hadronic matter in Nature, regardless of the direction in which we might explore the QCD phase diagram: temperature, baryon density or isospin density.

Table 1 corroborates our conjecture for the DD2-MEV vs. hNJL hybrid EoS. The relative difference in the transition pressures $D = 2(p_{\text{trans}}^{(s)} - p_{\text{trans}}^{(b)}) / (p_{\text{trans}}^{(s)} + p_{\text{trans}}^{(b)})$ is at the level of 15% only. Using this correlation together with the largest measured radius for the compact object 4U 1724-307 we find a p_{trans} of about 80 MeV/fm^3 that per-

Table 1. The onset pressure p_{trans} for symmetric matter (s) and in beta equilibrated NS matter (b) for the DD2-MEV vs. hNJL hybrid EoS, and the relative difference $D = 2(p_{\text{trans}}^{(s)} - p_{\text{trans}}^{(b)})/(p_{\text{trans}}^{(s)} + p_{\text{trans}}^{(b)})$.

η_4	v [fm ³]	$p_{\text{trans}}^{(s)}$ [MeV/fm ³]	$p_{\text{trans}}^{(b)}$ [MeV/fm ³]	D %
5	6.0	65.54	56.01	15.68
6	6.5	61.49	52.82	15.17
7	7.0	58.13	50.38	14.28
8	7.5	55.13	47.89	14.04
9	8.0	52.63	45.98	13.49

fectly agrees with the transition pressure extracted from experimental data using a statistical model at low temperature and high density in [48].

Acknowledgements

We acknowledge the partial support by the COST Action MP 1304 "NewCompStar" for our international networking activities in preparing this article. This work received support from the Polish NCN under grant No. UMO-2014/13/ B/ST9/02621. D.E.A-C. and S.T. received support from the Heisenberg-Landau programme for scientist exchange between JINR Dubna and German Institutes. S. B. acknowledges partial support by the Croatian Science Foundation under Project No. 8799. D.B. was supported in part by the Hessian LOEWE initiative through HIC for FAIR.

References

1. P. Demorest, T. Pennucci, S. Ransom, M. Roberts and J. Hessels, *Nature* **467**, 1081 (2010).
2. E. Fonseca *et al.*, arXiv:1603.00545 [astro-ph.HE].
3. J. Antoniadis *et al.*, *Science* **340**, 6131 (2013).
4. T. Klähn, D. Blaschke, F. Sandin, C. Fuchs, A. Faessler, H. Grigorian, G. Röpke and J. Trümper, *Phys. Lett. B* **654**, 170 (2007).
5. T. Klähn, R. Lastowiecki and D. B. Blaschke, *Phys. Rev. D* **88**, 085001 (2013).
6. C. Hoyos, D. Rodriguez Fernandez, N. Jokela and A. Vuorinen, *Phys. Rev. Lett.* **117**, no. 3, 032501 (2016).
7. T. Kojo, *Eur. Phys. J. A* **52**, no. 3, 51 (2016).
8. T. Schäfer and F. Wilczek, *Phys. Rev. Lett.* **82**, 3956 (1999).
9. T. Hatsuda, M. Tachibana, N. Yamamoto and G. Baym, *Phys. Rev. Lett.* **97**, 122001 (2006).
10. H. Abuki, G. Baym, T. Hatsuda and N. Yamamoto, *Phys. Rev. D* **81**, 125010 (2010).
11. M. Baldo, G. F. Burgio and H.-J. Schulze, in: *Superdense QCD Matter and Compact Stars*, Springer, Heidelberg, 2006, p.113.
12. M. Alford, M. Braby, M. W. Paris and S. Reddy, *Astrophys. J.* 629, 969 (2005).
13. R. Lastowiecki, D. Blaschke, H. Grigorian and S. Typel, *Acta Phys. Polon. Supp.* **5**, 535 (2012).
14. J.L. Zdunik and P. Haensel, *Astron. Astrophys.* **551**, A61 (2013).
15. <https://heasarc.gsfc.nasa.gov/docs/nicer>
16. <http://www.ska.ac.za>
17. D. Alvarez-Castillo, A. Ayriyan, S. Benic, D. Blaschke, H. Grigorian and S. Typel, *Eur. Phys. J. A* **52**, no. 3, 69 (2016).
18. A. Ayriyan, D. E. Alvarez-Castillo, D. Blaschke and H. Grigorian, *J. Phys. Conf. Ser.* **668**, no. 1, 012038 (2016).
19. D. E. Alvarez-Castillo, A. Ayriyan, D. Blaschke and H. Grigorian, eConf C140926 (2015).
20. A. Ayriyan, D. E. Alvarez-Castillo, D. Blaschke, H. Grigorian and M. Sokolowski, *Phys. Part. Nucl.* **46**, no. 5, 854 (2015).
21. D. Alvarez-Castillo, A. Ayriyan, D. Blaschke and H. Grigorian, arXiv:1408.4449
22. D. B. Blaschke, H. A. Grigorian, D. E. Alvarez-Castillo and A. S. Ayriyan, *J. Phys. Conf. Ser.* **496**, 012002 (2014).
23. R. C. Tolman, *Phys. Rev.* **55**, 364 (1939).
24. J. R. Oppenheimer and G. M. Volkoff, *Phys. Rev.* **55**, 374 (1939).
25. S. Typel, *Eur. Phys. J. A* **52**, 16 (2016).
26. M. G. Alford, S. Han and M. Prakash, *Phys. Rev. D* **88**, 083013 (2013).
27. D. E. Alvarez-Castillo and D. Blaschke, arXiv:1304.7758
28. D. E. Alvarez-Castillo and D. Blaschke, PoS CPOD 2014 (2015) 045.
29. B. K. Agrawal and S. K. Dhiman, *Phys. Rev. D* **79**, 103006 (2009).
30. B. K. Agrawal, *Phys. Rev. D* **81**, 023009 (2010).
31. D. Blaschke, S. Fredriksson, H. Grigorian, A. M. Öztas and F. Sandin, *Phys. Rev. D* **72**, 065020 (2005).
32. M. Prakash, J. R. Cooke and J. M. Lattimer, *Phys. Rev. D* **52**, 661 (1995).
33. S. Benic, D. Blaschke, D. E. Alvarez-Castillo, T. Fischer and S. Typel, *Astron. Astrophys.* **577**, A40 (2015).
34. S. Benic, *Eur. Phys. J. A* **50**, 111 (2014).
35. G. A. Contrera, A. G. Grunfeld and D. B. Blaschke, *Phys. Part. Nucl. Lett.* **11**, 342 (2014).
36. S. Benic, D. Blaschke, G. A. Contrera and D. Horvatic, *Phys. Rev. D* **89**, 016007 (2014).
37. M. B. Parappilly *et al.*, *Phys. Rev. D* **73**, 054504 (2006).
38. W. Kamleh *et al.*, *Phys. Rev. D* **76**, 094501 (2007).
39. O. Kaczmarek *et al.*, *Phys. Rev. D* **83**, 014504 (2011).
40. D. Blaschke, D. E. Alvarez-Castillo, S. Benic, G. Contrera and R. Lastowiecki, PoS ConfinementX , 249 (2012).
41. D. Blaschke, D. E. Alvarez-Castillo and S. Benic, PoS CPOD 2013 (2013), 063
42. C. J. Horowitz, E. J. Moniz and J. W. Negele, *Phys. Rev. D* **31**, 1689 (1985).
43. G. Röpke, D. Blaschke and H. Schulz, *Phys. Rev. D* **34**, 3499 (1986).
44. D. E. Alvarez-Castillo, M. A. R. Kaltenborn and D. Blaschke, *J. Phys. Conf. Ser.* **668**, 012035 (2016).
45. A. S. Khvorostukin, V. V. Skokov, V. D. Toneev and K. Redlich, *Eur. Phys. J. C* **48**, 531 (2006).
46. N. Yasutake, R. Lastowiecki, S. Benic, D. Blaschke, T. Maruyama and T. Tatsumi, *Phys. Rev. C* **89**, 065803 (2014).
47. D. E. Alvarez-Castillo and D. Blaschke, *Phys. Part. Nucl.* **46**, 846 (2015).
48. M. Petran and J. Rafelski, *Phys. Rev. C* **88**, 021901 (2013).

- 49. J. Rafelski and M. Petran, Acta Phys. Polon. Supp. **7**, 35 (2014).
- 50. V. F. Suleimanov, J. Poutanen, D. Klochkov and K. Werner, Eur. Phys. J. A **52**, 20 (2016).
- 51. D. E. Alvarez-Castillo and S. Kubis, ASP Conf. Ser. **466**, 199 (2012).
- 52. A. Bazavov *et al.* [HotQCD Collaboration].Phys. Rev. D **90**, 094503 (2014).
- 53. D. Blaschke, D. E. Alvarez-Castillo and T. Klähn, arXiv:1604.08575
- 54. M. Bejger, private communication.